RAPID COMMUNICATIONS IN MASS SPECTROMETRY
Rapid Commun. Mass Spectrom. 2005; **19**: 57–71
Published online in Wiley InterScience (www.interscience.wiley.com). DOI: 10.1002/rcm.1746

RCM

Automated immobilized metal affinity chromatography/nano-liquid chromatography/electrospray ionization mass spectrometry platform for profiling protein phosphorylation sites

Scott B. Ficarro*, Arthur R. Salomon, Laurence M. Brill, Daniel E. Mason, Michelle Stettler-Gill, Ansgar Brock and Eric C. Peters

Genomics Institute of the Novartis Research Foundation, 10675 John Jay Hopkins Drive, San Diego, CA 92121, USA

Received 23 August 2004; Revised 23 October 2004; Accepted 1 November 2004

A versatile integrated system has been developed for the automated enrichment and analysis of phosphopeptides by immobilized metal affinity chromatography/nano-liquid chromatography/electrospray ionization mass spectrometry (IMAC/nano-LC/ESI-MS). This system utilizes two independently controlled high-performance liquid chromatography (HPLC) pumps, an autosampler and microvalves to prepare and elute samples into an ion trap mass spectrometer. The use of robust reversed-phase HPLC columns with integrated ESI emitter tips enables the reproducible detection and identification of low-femtomole quantities of phosphopeptides. The entire system is coordinated through a simple user interface by customized software. The ruggedness of the system is demonstrated by highly reproducible analyses of single and multi-protein digests, while its utility is demonstrated by the thorough evaluation of the relative immunoprecipitation efficiencies of several commercially available anti-phosphotyrosine antibodies. Copyright © 2004 John Wiley & Sons, Ltd.

Reversible phosphorylation is a key mechanism by which cells regulate protein function.[1–3] For example, changes in the phosphorylation state of a protein can affect its activity, stability, cellular localization and interacting partners, and thus enable the dynamic fine-tuning of important cellular processes such as growth, differentiation and transcription.[4] In order to understand how phosphorylation regulates such processes, it is important to determine not only which proteins are indeed phosphorylated, but also to define their site(s) of modification as well as how they change over time.

Over the past decade, mass spectrometry has emerged as a powerful tool for the characterization of phosphorylated proteins.[3,5] Typically, individual proteins are first purified using affinity chromatography or two-dimensional (2D) gel electrophoresis, digested with a proteolytic enzyme, and analyzed by matrix-assisted laser desorption/ionization (MALDI-MS) or electrospray ionization mass spectrometry (ESI-MS). This strategy has been applied to identify proteins that change their phosphorylation state in response to various cellular perturbations.[6,7] However, the identification of specific sites of phosphorylation is far more challenging, as sub-stoichiometrically modified peptides are often difficult to detect among the higher intensity signals typically resulting from unmodified species.[5] In order to overcome this problem, an enrichment strategy selective for phosphopeptides such as immobilized metal affinity chromatography (IMAC) may be utilized.[8] This technique coupled with ESI-MS has demonstrated great success in the identification of phosphorylation sites from samples consisting of single proteins[3,9–12] or even complex mixtures.[13–18] However, the manual implementation of IMAC/nano-LC/ESI-MS experiments is laborious, requiring the ordered delivery of numerous chemical solutions as well as various microcapillary column manipulations, and thus, the technique can be difficult to apply to large numbers of in-gel digests or the multiple time point samples required to characterize rapid phosphorylation cascades.[18] Although automated IMAC/LC/ESI-MS approaches have been described,[10,19] these systems utilized flow rates of 5 μL/min and 1 mL/min, respectively, and therefore did not achieve the increased ESI sensitivity made possible by the use of micrometer scale emitter tips and low nL/min flow rates.[20–24] Such sensitivity is essential for the detection of phosphorylated peptides of low abundance. Additionally, these systems were limited to the use of particular LC and MS instruments controlled by a single manufacturer's software system.

Here we describe a strategic, robust integration of microcapillary IMAC enrichment[10,13,17] with recently described nano-LC/ESI-MS methodology.[23] The system is fully controlled from a simple user interface and is compatible with a variety of LC and MS instrumentation. In addition, the platform is versatile, allowing users to perform nano-LC/ESI-MS experiments with or without IMAC enrichment from

*Correspondence to: S. B. Ficarro, Genomics Institute of the Novartis Research Foundation, 10675 John Jay Hopkins Drive, San Diego, CA 92121, USA.
E-mail: sficarro@gnf.org

the same analysis list. Moreover, other 2D chromatographic separations schemes can readily be implemented by substituting the IMAC column with the appropriate stationary phase (i.e. strong cation- or anion-exchange media). The system has been used to identify protein phosphorylation sites from various samples containing individual proteins or more complex mixtures. Additionally, the automated nature of the system was employed to thoroughly evaluate the relative immunoprecipitation efficiencies of several commercially available anti-phosphotyrosine antibodies.

EXPERIMENTAL

Chemicals

HPLC-grade acetonitrile was purchased from Fisher Scientific (Pittsburgh, PA, USA). Angiotensin II phosphate (DRVpYIHPF) was from Calbiochem-Novabiochem (San Diego, CA, USA). Unless otherwise noted, all other chemicals, peptides, and proteins were obtained from Sigma-Aldrich (St. Louis, MO, USA).

Peptide synthesis

The peptide LIEDAEpYTAK was synthesized using FastMoc chemistry on an ABI 431A peptide synthesizer (Applied Biosystems, Foster City, CA, USA) using Fmoc-protected amino acids and Fmoc-Lys(Boc)-Wang resin (Calbiochem-Novabiochem). The peptide was cleaved from the resin using 95% trifluoroacetic acid/2.5% triisopropylsilane/2.5% water for 2 h, purified by preparative reversed-phase HPLC, and lyophilized.

Standard protein digests

Bovine serum albumin (BSA) was reconstituted in 8 M urea, 100 mM NH_4HCO_3 buffer, pH 8.0. Tris-carboxyethyl phosphine was added to a final concentration of 10 mM, and the mixture incubated at room temperature for 10 min. Iodoacetamide was then added to a final concentration of 20 mM, and alkylation allowed to proceed at room temperature for 45 min in the dark. The mixture was diluted with an equal volume of 100 mM NH_4HCO_3 buffer, pH 8.0, and digested with modified trypsin (Promega, Madison, WI, USA) for 8 h at 37°C. α-Casein was digested in a similar fashion, except that urea was not added.

Cell culture and immunoprecipitation

Cell culture was performed as described.[17] Briefly, Jurkat (clone E6) T cells were grown in RPMI 1640 medium with 10% fetal bovine serum (FBS), 2 mM L-glutamine, 100 μg/mL streptomycin sulfate, and 100 U/mL penicillin G, in a 5.0% CO_2 incubator at 37°C. Cells were treated with sodium pervanadate to inhibit tyrosine phosphatases and thus elevate overall levels of phosphotyrosine.[25] Cells ($\sim 1 \times 10^9$) were washed with RPMI lacking FBS at 4°C and then lysed for 20 min with rotation at 4°C in 25 mL of lysis buffer [20 mg/mL aprotinin, 20 mg/mL leupeptin, 50 mM Tris buffer pH 7.5, 100 mM NaCl, 1% Nonidet P-40, 10% glycerol, 1 mM Pefabloc (Fluka), 2 mM Na_3VO_4, 10 mM β-glycerophosphate (Ser/Thr phosphatase inhibitor) and 1 mM EDTA].

Lysates were centrifuged at 12 000 *g* for 15 min at 4°C. LIEDAEpYTAK (50 pmol per $\sim 1 \times 10^9$ cell equivalents) and immobilized anti-phosphotyrosine antibodies (clone PT66, Sigma-Aldrich; clone pY20, Sigma-Aldrich; or clone 4G10, Upstate Biotechnology, Charlottesville, VA, USA; 150 μL resin/$\sim 1 \times 10^9$ cell equivalents) were added to the supernatant for 4 h at 4°C with rotation. Beads were washed once with 50 mL of ice-cold lysis buffer and once with 50 mL of 20 mM Tris buffer, pH 7.4, 120 mM NaCl. Proteins were recovered from the beads with 100 mM NH_4HCO_3 buffer, pH 8.3, 8 M urea for 5 min at 96°C and the supernatant was filtered using PVDF membranes with a pore size of 0.22 μm (Millipore Inc., Bedford, MA, USA). The mixture was diluted with an equal volume of water and proteins were digested overnight with 5 μg of modified trypsin (Promega) at 37°C. Tryptic peptides were desalted and methylated as described.[17,18]

Construction of desalting, IMAC, and precolumns

Fused-silica tubing (360 μm o.d. × 200 μm i.d.; Polymicro Technologies, Phoenix, AZ, USA) was fritted using a procedure modified from Cortes *et al*.[26] Capillaries were dipped into a solution of 5:1 KASIL® No. 1 (PQ Corporation, Valley Forge, PA, USA; 2.5:1 SiO_2/K_2O)/formamide and placed in an oven at 100°C for 2 h. Frits were cut to the desired length (ca. 1–2 mm) and then rinsed with 9:1 acetonitrile/isopropanol, followed by 0.1% acetic acid. Fritted tubing was packed with either 12 cm of POROS 10R2 (Perseptive Biosystems, Framingham, MA, USA) for desalting columns or 15 cm of POROS 20MC (Perseptive Biosystems) for IMAC columns using a pressure bomb. Packed columns were mounted into microinjection valves (UpChurch Scientific, Oak Harbor, WA, USA) according to the manufacturer's instructions. Precolumns (360 μm o.d. × 75 μm i.d.) were fritted and rinsed as described above and packed with 2 cm of 5 μm Monitor C18 particles (Column Engineering, Ontario, CA, USA).

Construction of analytical columns

Analytical columns with integrated ESI emitter tips were constructed by first pulling a 4–5 μm i.d. emitter tip on 360 μm o.d. x 75 μm i.d. fused silica using a P-2000 laser puller (Sutter Instruments, Novato, CA, USA) with the following parameters: Heat = 290, Filament = 0, Velocity = 15, Delay = 127, Pull = 10. Tips were fritted with a water slurry of 3 μm silica particles (Bangs Laboratories Inc., Fishers, IN, USA) by using a pressure bomb to pack 1–2 mm of particles into the tip. After fritting, columns were packed with 12 cm of 5 μm Monitor C18.

Automated IMAC/nano-LC/ESI-MS system overview

To automate IMAC and nano-LC/ESI-MS, the platform shown in Fig. 1(A) was interfaced to an ion trap mass spectrometer. Samples were introduced with an HPLC pump and microautosampler (models G1376A and G1389A, respectively, Agilent Technologies, Palo Alto, CA, USA). The autosampler was fitted with a sample loop (1/16″ o.d. × 0.02″ i.d., volume 60 μL) cut from PEEK tubing (UpChurch Scientific). Microinjection valves (UpChurch Scientific) enabled independent switching of microcapillary desalting and IMAC columns into the flow path, and thus enrichment of samples prior to nano-LC/ESI-MS (Fig. 1(A), valves 1 and 2). An

additional valve (Fig. 1(A), valve 3) switched flow between waste and a vented column μESI source similar to that described by Licklider *et al*.[23] Opening of the vent with valve 4 (mounted on the mass spectrometer, Fig. 1(B)) allowed samples to be loaded onto the precolumn at a flow rate of 4 μL/min. Vent closure created a channel for HPLC solvent splitting (Fig. 1(C)), allowing gradient elution of peptides with a second HPLC pump (model G1376A; Agilent Technologies) into a quadrupole ion trap mass spectrometer (LCQDecaXP; Thermo Electron, San Jose, CA, USA) at flow rates less than 100 nL/min. This scheme enables simultaneous sample preparation and MS analysis and also prevents contamination of the μESI fluidic system with the reagents utilized for IMAC column activation.

System software/communication

All instruments were controlled from a single computer running the Windows 2000 operating system (Microsoft, San Diego, CA, USA). The HPLC pumps and mass spectrometer were controlled by separate processes of Chemstation software version 10.0.1 (Agilent Technologies) and Xcalibur version 1.3 (Thermo Electron), respectively. Chemstation and Xcalibur

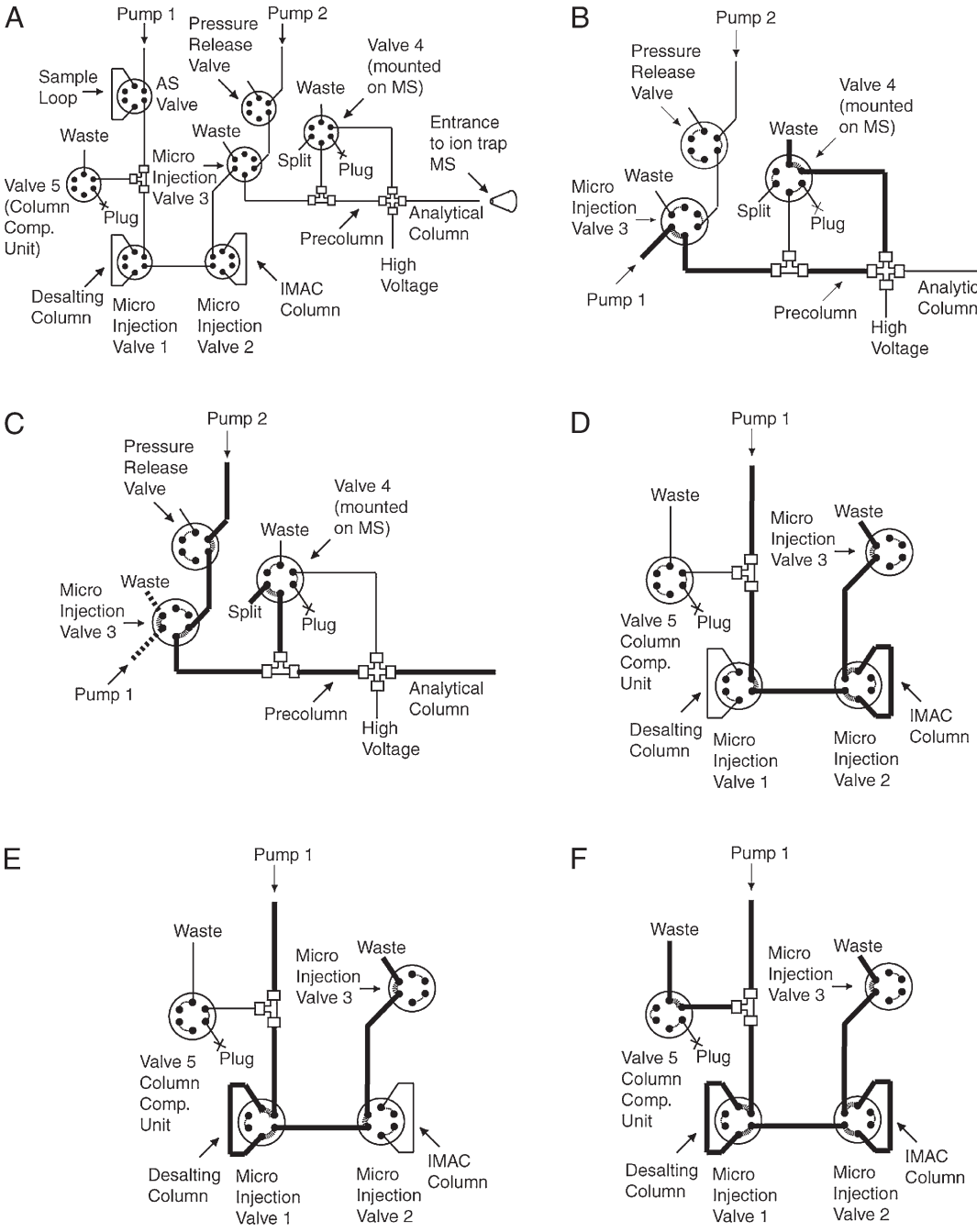

Figure 1. (A) Schematic showing fluidic system components utilized for automated analysis of phosphorylated peptides. AS, autosampler, Comp., compartment. Valve configuration (depicted with arcs) and flow paths (bold lines) for (B) loading a sample onto the precolumn, (C) gradient elution of peptides into the mass spectrometer, (D) activation of the IMAC column, (E) loading a sample onto the desalting column, and (F) gradient elution of peptides to the IMAC column.

processes were controlled with Auto-Mate Analysis Control software (AACS), developed in-house and coded in Visual Basic 6.0 (Microsoft). AACS allows users to specify experimental parameters (i.e. experiment type, injection volume, vial position and both HPLC and MS methods) and to execute a list of experiments. Since both pumps were controlled independently, IMAC enrichment and nano-LC/ESI-MS analysis of separate samples occurred simultaneously.

Intermodule communication was achieved as shown in Fig. 2. The PC was equipped with two network cards (DFE-530TX + PCI Adapter; D-Link Systems, Fountain Valley, CA, USA), one of which was dedicated to communication with the HPLC systems. The first HPLC system consisted of the autosampler, pump 1, and a column compartment unit (G1316A; Agilent Technologies). The second HPLC system consisted of pump 2 and a valve (G1158A; Agilent Technologies). Agilent modules were interconnected through cable area networks (CANs). Contact closure events were used to control actuation of valves 1, 2 and 3, and also to deliver start signals to the mass spectrometer and pump 2 (external contacts board; Agilent Technologies, part No. G1351A).

nano-LC/ESI-MS experiments

Samples were injected from 2.0 mL skirted microcentrifuge tubes (Sarstedt, Newton, NC, USA) that were first razor cut to fit the autosampler and then sealed with 11 mm crimp caps. For limiting volume inserts, 0.2 mL PCR tubes (Abgene, Rochester, NY, USA) were placed inside 2.0 mL skirted microcentrifuge tubes that were cut and crimp cap sealed. To perform nano-LC/ESI-MS experiments, AACS software loaded user-specified methods into Chemstation process 2 (controlling the gradient delivery pump) and Xcalibur 1.3. AACS then activated a sequence of steps for sample loading with Chemstation process 1 (controlling the sample loading pump). This sequence opened the vent (Fig. 1(B), valve 4) and loaded peptides onto the precolumn at a flow rate of 4 μL/min. It should be noted that flow rates significantly greater than 4 μL/min can result in loss of hydrophilic peptides.[23] After sample loading, valve 3 was switched, and the gradient delivery pump and mass spectrometer were activated by contact closure. Valve 4 was then switched to close the vent and create a channel for flow splitting (Fig. 1(C)). Peptides were eluted to the mass spectrometer using a linear gradient and a flow rate of approximately 100 nL/min (measured at the emitter tip). HPLC solvents consisted of aqueous 0.1 M acetic acid (solvent A), and acetonitrile with 0.1 M acetic acid (solvent B). For 'peak parking' experiments, the flow rate was dropped to approximately 30 nL/min as described below when peptides began to elute from the column.

IMAC/nano-LC/ESI-MS experiments

For IMAC experiments, AACS loaded an IMAC enrichment sequence into Chemstation process 1 (controlling the sample loading pump) and executed it. This sequence positioned valves as shown in Fig. 1(D) and stripped and activated the IMAC media with reagents via the following autosampler injections, all performed at a flow rate of 35 μL/min (typical backpressure 60 bar): 2 × 40 μL of 50 mM EDTA (pH 8.0), 1 × 40 μL of water, 3 × 40 μL of 100 mM iron(III) chloride, and 1 × 40 μL of 0.1% acetic acid. Samples were then loaded onto the column at a flow rate of 2.5 μL/min, and rinsed with 2 × 40 μL of 25:74:1 (v/v/v) acetonitrile/water/acetic acid containing 100 mM NaCl, followed by 1 × 40 μL of 0.1% acetic acid. Valve 3 was positioned to direct flow delivered by

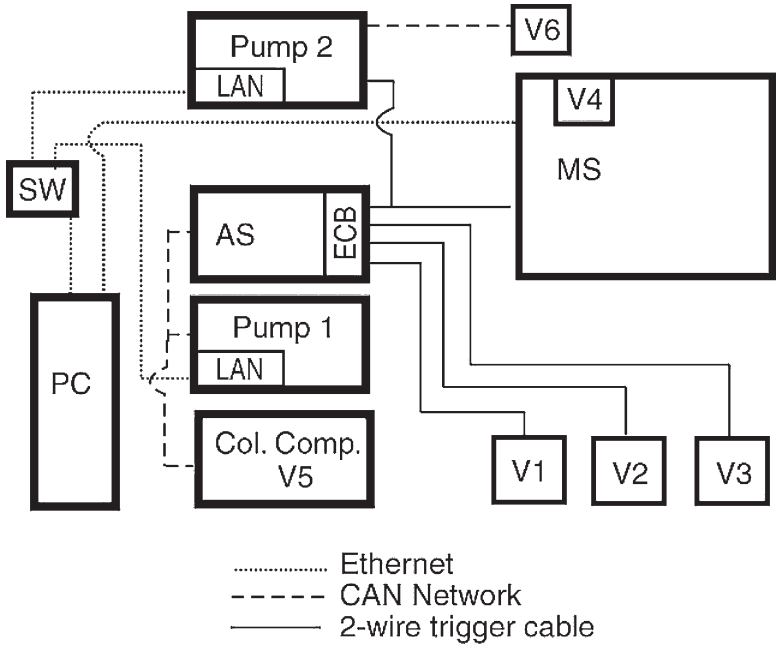

Figure 2. Diagram showing intermodule communication scheme for automated peptide desalt/IMAC/nano-LC/ESI-MS system. V, valve; LAN, local area network card; ECB, external contacts board; SW, ethernet switch; AS, autosampler; PC, personal computer; MS, ion trap mass spectrometer; CAN, cable area network; Col. Comp., column compartment unit.

HPLC pump 1 to waste so that these reagents did not contaminate the μESI fluidic system. After execution of this sequence, AACS software loaded user-specified methods into Chemstation process 2 (controlling the gradient delivery pump) and Xcalibur 1.3 (controlling the mass spectrometer). Then, a sequence of steps for phosphopeptide elution from the IMAC column to the precolumn was started by Chemstation process 1 (controlling the sample loading pump). To elute phosphopeptides, the IMAC column was switched out of the flow path, and the autosampler injected 40 μL of 50 mM Na_2HPO_4 buffer, pH 9.0, at a flow rate of 20 μL/min. After 1 min, the IMAC column was switched in-line and valve 3 was switched to direct flow to the precolumn (Fig. 1(B)). The method was programmed such that a volume of 12–14 μL of the Na_2HPO_4 buffer was washed over the IMAC column and the precolumn. After phosphopeptide elution, valve 3 was switched, and the gradient delivery pump (pump 2, Fig. 1(A)) was activated by contact closure, triggering a short precolumn wash with solvent A (approximately 10 μL at 80 bar) to remove Na_2HPO_4 buffer. After desalting, pressure was released through an additional valve (Fig. 1(A), 'Pressure Release Valve') and peptides were gradient-eluted to the mass spectrometer as described above.

Desalt-IMAC/nano-LC/ESI-MS experiments

To desalt samples prior to IMAC enrichment, AACS first loaded a sequence on Chemstation process 1 (controlling the sample loading pump). This sequence stripped and activated the IMAC resin as described above, but then switched the IMAC column out of the flow path. Samples were loaded onto the desalting column (Fig. 1(E)) and rinsed with solvent A at a flow rate of 10 μL/min. Following desalting, valves were positioned as shown in Fig. 1(F), and the loading pump eluted peptides to the IMAC column with an HPLC gradient (0–70% solvent B in 17 min) at a flow rate of 1.5 μL/min. After gradient elution, the desalting column was switched out of line, and the IMAC column was rinsed with 2 × 40 μL of 25% 25:74:1 acetonitrile/water/acetic acid containing100 mM NaCl, followed by 1 × 40 μL of 0.1% acetic acid (Fig. 1(D)). Elution to the precolumn and MS analysis of peptides were then performed as described above.

Parameters for operating the ion trap mass spectrometer

MS methods were created with Xcalibur 1.3 software and consisted of four segments. The first and last segments specified a spray voltage of 0 V, so that voltage was not applied to the emitter tip without flow. The second segment specified a spray voltage of 1.8 kV and a sheath gas flow of 30 to generate the electrospray and to disperse the liquid droplet from the emitter. The third segment contained parameters for MS analysis. For tandem mass spectrometry (MS/MS) experiments, collision energy was set to 35% (3 Da window; precursor m/z ±1.5 Da). For data-dependent scanning, dynamic exclusion was specified with a repeat count of one and an exclusion time of 1.5 min.

Database analysis

MS/MS spectra were assigned to peptide sequences from the NCBI non-redundant protein database using Bioworks 3.1SR1 (Thermo Electron) and the SEQUEST algorithm.[27] Search parameters specified a differential modification of +80 Da to serine, threonine, and tyrosine residues (phosphorylation) and a static modification of +17 Da to glutamic acid, aspartic acid, and the C-terminus (deuterated methyl ester) when applicable. All phosphopeptide sequences were manually verified.

RESULTS AND DISCUSSION

Nano-LC/ESI-MS performance

In order to perform automated phosphopeptide analysis, the platform shown in Fig. 1(A) was interfaced to an ion trap mass spectrometer. This platform differs significantly from previously described automated nano-LC/ESI-MS systems.[22,23] For example, microinjection valves enabled the facile switching of capillary desalting or IMAC columns into the flow path. In addition, separate precolumns and analytical columns were utilized rather than a continuous 'vented' column,[23] while the analytical columns employed laser pulled tips (4–5 μm i.d.) fritted with silica particles. To evaluate the chromatographic performance of the system, 1 μL of a 100 fmol/μL solution of a tryptic digest of BSA was injected directly onto the precolumn without IMAC enrichment and eluted into the mass spectrometer at a flow rate of 100 nL/min using an HPLC gradient of 0–70% solvent B in 17 min. Peak widths of the various BSA peptides averaged 12.5 s (measured at base) corresponding to peak elution volumes of approximately 21 nL (not shown). Signal- to-noise (S/N) ratios for these peptides were greater than 300:1 (not shown), demonstrating a level of performance similar to other nano-LC/ESI-MS systems.[23] These results were similar to those obtained in the absence of a vented column, by instead loading the same sample directly onto the precolumn with a pressure bomb (data not shown), indicating that the incorporation of additional valves for peptide enrichment did not significantly sacrifice sensitivity or chromatographic performance.

Although automated data-dependent MS/MS experiments and database searching identified numerous peptide sequences from the BSA tryptic digest using the above LC conditions (data not shown), it has been recognized that increased numbers of peptides can often be identified by peak parking, or lowering the flow rate, during the gradient elution of peptides.[24,28] This technique provides both more time for the mass spectrometer to perform MS/MS experiments[28] as well as increased ESI sensitivity.[21,22] To implement peak parking in an automated fashion, a 'scouting' analysis was first performed to establish the time at which to lower the flow rate. BSA tryptic peptides were eluted into the mass spectrometer at a constant flow rate of 100 nL/min using a slightly extended HPLC gradient to provide additional peptide separation (0–70% solvent B in 30 min). A peak parking method was then created by specifying a drop in flow rate from 100 nL/min to approximately 30 nL/min over a 30 s time interval that began at the retention time of the hydrophilic BSA tryptic peptide YIC*DNQDTISSK (C* = carboxyamidomethyl cysteine). Using this method, the average peak widths for BSA peptides increased from 14 to 35 s (measured at base), more than doubling the time available for the MS/MS analysis of a given species (Fig. 3).

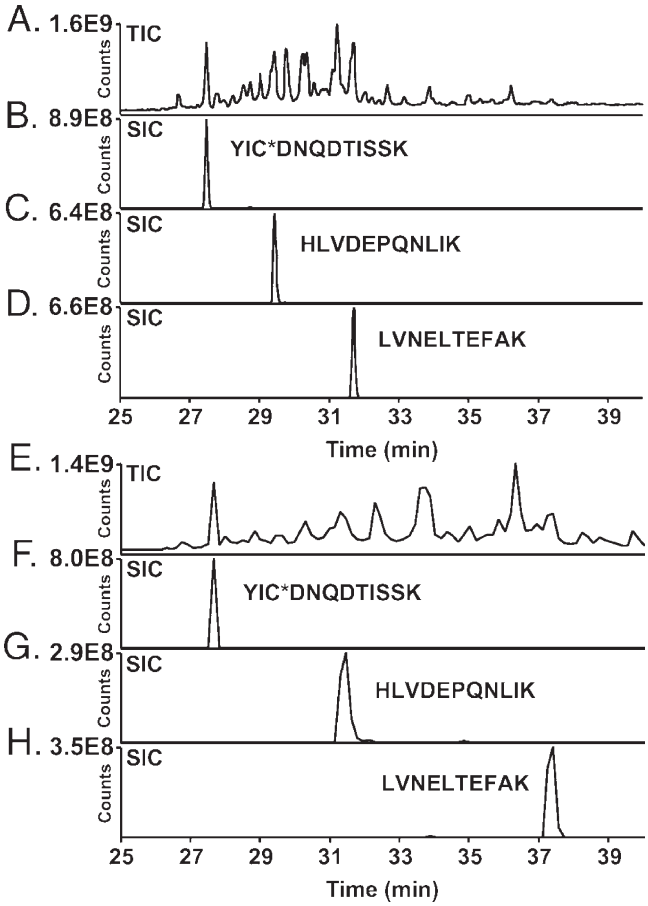

Figure 3. Peak parking was performed in an automated fashion, and increased peak widths of peptides. (A, E) Total ion chromatograms (TICs) and (B–D, F–H) selected ion chromatograms (SICs) for doubly charged peptide ions (B, F) YIC*DNQDTISSK (C* = carboxyamidomethyl cysteine), (C, G) HLVDEPQNLIK, and (D, H) LVNELTEFAK recorded during nano-LC/ESI-MS analysis of 1 μL (100 fmol) tryptic BSA peptides (A–D) with a constant 100 nL/min flow rate and (E–H) with peak parking, i.e. dropping the flow from 100 to 30 nL/min at the retention time of YIC*DNQDTISSK. Gradient parameters specified 0–70% solvent B in 30 min. The mass spectrometer acquired ESI mass spectra (*m/z* 300–2000).

Importantly, the 'scouting' analysis needed only to be performed when the precolumn or analytical column was changed, or after extended idle time. This robust implementation of peak parking shows minimal run-to-run differences in retention times and peak areas, and can readily be applied to the analysis of complex mixtures of phosphorylated peptides (see data below).

IMAC/nano-LC/ESI-MS

Next, we evaluated the ability of the system to perform IMAC/nano-LC/ESI-MS analyses. The synthetic tyrosine-phosphorylated peptide DRVpYIHPF (1 μL of a 100 fmol/μL solution) was injected onto an iron(III)-activated IMAC column, rinsed with 25:74:1 (v/v/v) acetonitrile/water/acetic acid containing 100 mM NaCl, and eluted to a reversed-phase precolumn in a completely automated fashion. The peptide was detected with a S/N ratio greater than 300:1, similar to the values observed when the same peptide was instead directly loaded onto the precolumn (data not shown). In order to demonstrate the reproducibility of the platform, 1 pmol of DRVpYIHPF was injected and analyzed five times using the IMAC/nano-LC/ESI-MS system. Each of these runs was preceded by the injection and nano-LC/ESI-MS analysis without IMAC enrichment of 1 pmol of angiotensin I injected from a separate vial, such that all ten experiments were executed from a single sample list. A concentration of 1 pmol was chosen in an effort to minimize adsorptive losses of peptide to the surface of the autosampler vial through the course of all ten analyses. As shown in Table 1, the peak areas for each peptide varied by less than 10%, while their retention times varied by less than 8 s, indicating that the peptides were analyzed in a reproducible, fully automated fashion. Additionally, independent control of the HPLC pumps used for sample loading and gradient elution enabled the IMAC enrichment of DRVpYIHPF to occur during the gradient elution of angiotensin I into the mass spectrometer, reducing the overall analysis time by approximately 35%.

To demonstrate the automated enrichment and sequencing of phosphorylated peptides from a protein digest, 1 μL of a 100 fmol/μL tryptic digest of α-casein was analyzed using a top 4 data-dependent MS/MS method on the described platform both without (Figs. 4(A)–4(D)) and with (Figs. 4(E)–4(H)) IMAC enrichment. Four phosphorylated peptides were

Table 1. Retention times (RT) and peak areas (area) for angiotensin I analyzed by nano-LC/ESI-MS (left column) and DRVpYIHPF analyzed by IMAC/nano-LC/ESI-MS (right column) in a fully automated fashion from a single sample list

Angiotensin I (nano-LC/ESI-MS)			DRVpYIHPF (IMAC/nano-LC/ESI-MS		
Analysis #	RT	Area	Analysis #	RT	Area
1	27.54	1.4×10^{10}	2	28.13	7.6×10^{9}
3	27.56	1.5×10^{10}	4	28.13	7.3×10^{9}
5	27.61	1.3×10^{10}	6	28.25	8.2×10^{9}
7	27.61	1.4×10^{10}	8	28.25	8.8×10^{9}
9	27.61	1.2×10^{10}	10	28.19	8.4×10^{9}
Mean	27.59	1.4×10^{10}	Mean	28.19	8.1×10^{9}
Std. Dev.[a]	0.034	1.1×10^{9}	Std. Dev.[a]	0.060	6.1×10^{8}
CV[b]	0.12%	8.4%	CV[b]	0.21%	7.5%

[a] Std. Dev., standard deviation.
[b] CV, coefficient of variation or relative standard deviation multiplied by 100%.

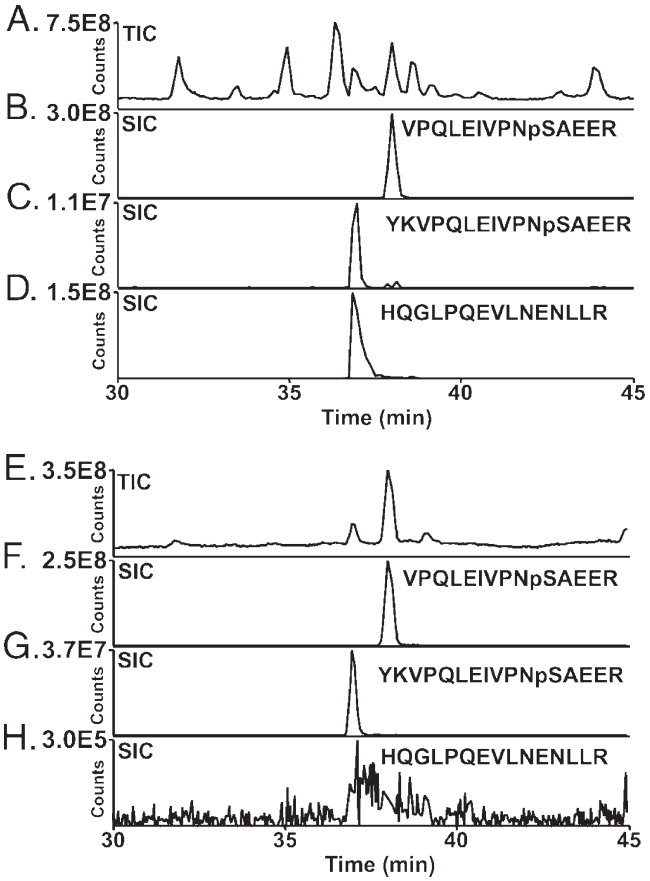

Figure 4. Fully automated IMAC/nano-LC/ESI-MS enrichment of phosphorylated peptides from a protein digest. (A, E) Total ion chromatograms (TICs) and (B–D, F–H) selected ion chromatograms (SICs) for doubly charged peptide ions (B, F) VPQLEIVPNpSAEER, (C, G) YKVPQLEIVPNpSAEER, and (D, H) HQGLPQEVLNENLLR recorded during nano-LC/ESI-MS analysis of 1 μL (100 fmol) tryptic α-casein peptides (A–D) without and (E–H) with IMAC enrichment. Gradient parameters specified 0–70% solvent B in 30 min with automated peak parking. The mass spectrometer performed cycles of one MS scan (*m/z* 300–2000), followed by data-dependent MS/MS scans of the four most abundant precursor ions detected in the initial MS scan. pS, phosphoserine residue.

identified and manually verified, including one arising from the contaminant protein β-casein (Table 2, right column). MS and MS/MS scans for two of the phosphopeptides are shown in Figs. 5(A)–5(D). The S/N ratio for the phosphopeptide from β-casein was relatively low (20:1, Fig. 5(A)), and it was only detected after IMAC enrichment (Table 2). Additionally, many non-phosphorylated peptides such as HQGLPQEVLNENLLR were no longer detected after IMAC (Table 2, Figs. 4(D) and 4(H)). To affect the enrichment of even lower quantities of phosphopeptide, 1 μL of a 10 fmol/μL tryptic digest of α-casein was injected and analyzed as above. The peptide VPQLEIVPNpSAEER was still detectable (Figs. 5(E) and 5(F)), and was correctly identified by SEQUEST. These results demonstrate that the system can affect the fully automated nano-scale IMAC enrichment of low-femtomole levels of phosphorylated peptides from single protein digests, and should thus be useful in a number of applications such as 2D gel-based phosphorylation studies.[6,7] Although acidic peptides will also most likely be enriched on the IMAC column under these conditions,[11,13,17] the overall net enrichment of phosphopeptides should still prove highly useful for the identification of phosphorylation sites on single proteins, and potentially from even more complex mixtures such as class I MHC peptide extracts[29] and plasma membrane shavings.[15] For the analysis of mixtures of even greater complexity, methyl ester modification of peptides has definitively been shown to reduce the undesired retention of acidic peptides, thus further increasing the selectivity of IMAC for phosphopeptides.[13,17]

Table 2. Peptides detected by automated nano-LC/ESI-MS (left column) or IMAC/nano-LC/ESI-MS (right column) analysis of 100 fmol (1 μL) α-casein tryptic digest

nano-LC/ESI-MS	IMAC/nano-LC/ESI-MS
Sequence	Sequence
HQGLPQEVLNENLLR	YKVPQLEIVPNpSAEER
YPSYGLNYYQQK	FQpSEEQQQTEDELQDK[a]
HQGLPQEVLNENLLR	TVDMEpSTEVFTK
ALNEINQFYQK	VPQLEIVPNpSAEER
VPQLEIVPNpSAEER	
YKVPQLEIVPNpSAEER	
YLGYLEQLLR	
VPQLEIVPNSAEER	
FFVAPFPEVFGK	
FALPQYLK	

[a] Peptide derived from β-casein.

Desalt/IMAC/nano-LC/MS

A recent study investigating the optimization of IMAC procedures for the broad-scale profiling of phosphorylation cascades demonstrated that desalting of the methyl ester modified peptide mixture prior to the IMAC enrichment step increased the recovery of phosphorylated peptides.[17] Therefore, it would be highly desirable to also incorporate this capability into any automated platform for wide-scale phosphorylation profiling. To demonstrate the feasibility of automated peptide desalt/IMAC/nano-LC/ESI-MS, 100 fmol of the synthetic peptide DRVpYIHPF was first injected onto a POROS10R2 column, washed, and eluted directly to the activated IMAC column using an HPLC gradient of 0–70% solvent B in 17 min. The IMAC enrichment process was performed as described above, and the retained fraction was eluted to the reversed-phase precolumn and subsequently gradient eluted into the mass spectrometer. DRVpYIHPF was detected with a S/N ratio similar to that observed when IMAC was performed without a desalting step or upon the direct injection of 100 fmol of DRVpYIHPF onto the precolumn (data not shown), demonstrating that minimal losses of peptide result from the additional automated desalting/IMAC enrichment steps.

Based on these encouraging results, automated desalt/IMAC/nano-LC/ESI-MS was extended to the phosphorylation analysis of highly complex peptide mixtures. Whole cell lysates of Jurkat cells (human T cell leukemia) stimulated with pervanadate were incubated with anti-phosphotyrosine antibodies (clone PT-66). The immunoprecipitated proteins

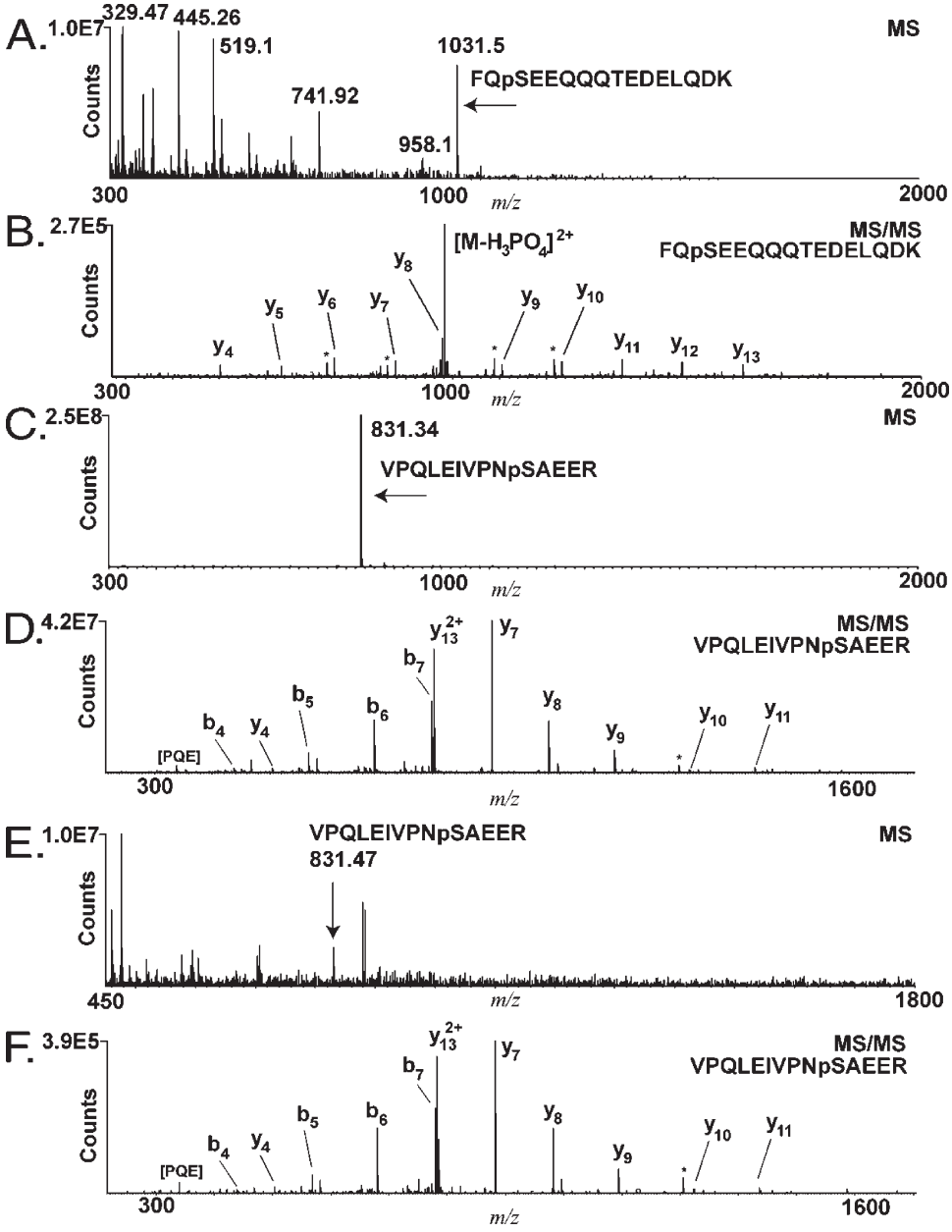

Figure 5. Representative MS and MS/MS spectra acquired during automated IMAC/nano-LC/ESI-MS analysis of 100 fmol (A–D) and 10 fmol (E, F) α-casein digest. Doubly charged ions of FQpSEEQQQTEDELQDK and VPQLEIVPNpSAEER were observed in MS spectra (A, C, E). Sequences and phosphorylation sites were identified by SEQUEST and manually verified (B, D, F). *, loss of water/ammonia.

were digested with trypsin, and the resulting peptides were methyl ester modified. Replicate desalt/IMAC/nano-LC/ESI-MS analyses of ca. 1×10^8 cell equivalents were performed using a top 4 data-dependent MS/MS method and automated peak parking. A blank desalt/IMAC/nano-LC/ESI-MS experiment was performed after the first analysis to evaluate sample carryover. These experiments resulted in the identification of 75 phosphopeptides containing 92 sites of phosphorylation, including 57 tyrosine phosphorylation sites on 34 different proteins (Table 3). Numerous phosphotyrosine-containing peptides arising from proteins known to play critical roles in T-cell signaling were identified (i.e. ZAP-70, CD3, PLCγ2), supporting the proposal that pervanadate treatment may mimic T-cell receptor ligation in Jurkat cells.[25] More than 85% of the phosphopeptides were observed in both analyses with run-to-run variations in peak area averaging 1.4-fold, indicating that this automated system can indeed reproducibly identify phosphorylation sites on cellular proteins from complex mixtures. The S/N ratio of the precursor ion signals for the remaining peptides were less than 5:1, resulting in their identification in only one of the two analyses. Importantly, even after analysis of this very complex mixture, little carryover was detected in the blank desalt/IMAC/nano-LC/ESI-MS analysis (Fig. 6), indicating complex peptide mixtures can be analyzed without significant carryover.

Table 3. Peptide sequences with assigned phosphorylation sites identified from clone PT-66 immunoprecipitates of pervanadate-stimulated Jurkat cells using automated desalt/IMAC/nano-LC/ESI-MS

Sequence[a]	Protein name	Accession[b]	RT analysis 1[c]	RT analysis 2[c]	Area analysis 1[d]	Area analysis 2[d]	Fold difference[e]	MS/MS, 1[f]	MS/MS, 2[f]
MYPPRpSPK	A2LP	27 262 649	32.11	32.15	1.7E+08	1.8E+08	0.9	*	*
KHpSPpSPPPPTPTESR	SWI/SNF complex	1 549 239	32.3	32.32	2.1E+08	2.2E+08	1.0	*	*
DKDAYpSSFGSR	Hbox-3, Y linked	13 514 809	33.15	32.98	9.2E+07	8.4E+07	1.1	*	
NHpSPLPPPQTNHEEPSR	Iymphocyte cytosolic protein 2	5 031 855	33.15	33.15	1.4E+08	1.5E+08	0.9	*	
FIHQQPQSSpSPVpYGSSAK	paxillin	4 506 345	33.5	33.51	1.0E+08	1.1E+08	0.9	*	*
RYPSSIpSSpSPQK	NICE-4 protein	13 111 995	33.5	33.51	4.7E+08	4.7E+08	1.0	*	*
YDERPGPpSPLPHR	U1 snrp 70 kDa	29 568 103	33.5	33.86	1.2E+08	1.4E+08	0.9	*	*
RHpTDPVQLQAAGR	GADS	4 758 476	34.51	34.67	3.1E+08	5.7E+08	0.5	*	*
p(SSGS)PYGGGYGSGGGSGGYGSR	ROA3_HUMAN	1 710 627	36.13	36.13	2.7E+07	5.8E+07	0.5	*	*
PGGYGYGpYGR	RNA Binding Motif Protein 3	5 803 137	ND	36.32	ND	4.60E+07	NA		*
RYPSSISSpSPQKDLTQAK	NICE-4 protein	1 311 195	37.26	37.49	8.7E+07	1.8E+08	0.5	*	*
GHDLpYQGLSTATK	CD3 zeta	4 557 431	38.47	38.45	1.9E+08	2.5E+08	0.8	*	*
VHQLYEpTIQR	Dynactin complex 50 kDa subunit	22 096 346	38.65	38.81	2.3E+07	4.0E+07	0.6	*	*
SPAVATSTAAPPPPpSSPLPSK	NICE-4 protein	13 111 995	38.84	38.63	5.0E+07	8.2E+07	0.6	*	*
GFGGQpYGIQK	Lyn Substrate 1	4 885 405	38.84	38.81	6.3E+07	1.4E+08	0.5	*	*
DLpYSGLNQR	CD3 epsilon	4 502 671	39.02	39	7.4E+07	7.9E+07	0.9	*	*
TpYQASSAAFR	similar to KIAA0280	20 482 720	39.02	39	3.6E+07	5.2E+07	0.7	*	*
pYNTGGNPTEDVSVNSR	FYN-Binding Protein	4 503 821	39.93	40.13	7.5E+07	6.2E+07	1.2	*	*
RIDTLNSDGpYTPEPAR	ZAP-70	1 177 044	40.69	ND	3.5E+07	ND	NA	*	
SAVGHEpYVAEVEK	Lyn Substrate 1	4 885 405	41.99	42	9.0E+07	4.7E+07	1.9	*	*
KNPQEGLpYNELQK	CD3 zeta	4 557 431	42.34	42.35	5.0E+07	2.3E+07	2.2	*	*
ARPATDSFDDpYPPR	eukaryotic TIF 4B	4 503 533	42.71	ND	3.4E+07	ND	NA	*	
LDQPVpSAPPpSPR	H4	22 477 628	42.23	42.71	2.4E+08	1.6E+08	1.5	*	*
p(STT)PPPAEPVSLPQEPPKPR	Ras-GAP SH3 binding protein	3 098 601	43.23	42.9	2.3E+08	1.2E+08	1.9	*	*
NEEGKpYGpYVLR	FYN binding protein	4 503 821	43.23	43.1	4.2E+07	3.0E+07	1.4	*	
AELGSQEGpYVPK	GADS	4 758 476	43.07	43.42	9.0E+07	8.4E+07	1.1	*	*
FQDVGPQAPVGSVpYQK	HIP-55	21 361 670	43.61	43.44	6.1E+07	5.7E+07	1.1	*	*
TQpTPPVpSPAPQPTEER	Cortactin	2 498 954	43.79	43.44	4.8E+08	4.0E+08	1.2	*	*
LGEpYEDVSR	TBCB	3 023 518	ND	43.62	ND	6.10EE+07	NA		*
LIEDNEpYTAR	Lck Kinase	6 984 209	44.15	43.99	1.0E+08	9.2E+07	1.1	*	*
pYGYVLR	FYN binding protein	4 503 821	44.16	44.15	1.6E+08	1.9E+08	0.8	*	*
EpYVNVSQELHPGAAK	LAT	7 657 293	44.15	44.33	7.1E+07	7.4E+07	1.0		*
ALGADDSpYpYTAR	ZAP-70	1 177 044	44.5	43.99	2.3E+08	2.1E+08	1.1	*	*
YYEGYpYAAGPGYGGR	LIM domain containing	5 031 887	44.5	44.16	1.1E+08	6.1E+07	1.8	*	
ARApSFPDQApYANSQPAAS	SIT	7 657 577	44.68	43.99	2.9E+08	3.4E+08	0.9	*	*
IDTLNpSDGpYTPEPAR	ZAP-70	1 177 044	44.33	44.5	1.1E+08	1.3E+08	0.8	*	*
YIEDEDpYpYKASVTR	FAX	1 165 219	45.1	45.41	5.8E+07	3.0E+07	1.9	*	*
DINSLpYDVSR	Phospholipase C, gamma 2	4 505 871	45.41	45.1	4.4E+07	2.6E+07	1.7	*	*
IKPSSpSANAIpYSLAAR	CBL	6 680 858	45.79	45.43	6.8E+07	7.6E+07	0.9	*	*
SQpYEVFR	Hypothetical protein PRO0971	21 361 757	45.97	45.9	3.0E+07	4.1E+07	0.7		*
LVNEAPVYSVpYSK	STAM2	21 265 031	ND	46.08	ND	3.00E+07	NA		*
YYEGpYpYAAGPGYGGR	LIM domain containing	5 031 887	46.33	45.9	5.1E+07	4.9E+07	1.0	*	*

Continues

Table 3. Continued

Sequence[a]	Protein name	Accession[b]	RT analysis 1[c]	RT analysis 2[c]	Area analysis 1[d]	Area analysis 2[d]	Fold difference[e]	MS/MS, 1[f]	MS/MS, 2[f]
pYADLPGIAR	p50 dynamitin	28 274 444	46.69	46.26	5.1E+07	5.8E+07	0.9	*	*
SGSpYSYLEER	protein phosphatase 1	4 505 317	46.69	46.44	5.5E+07	6.2E+07	0.9	*	*
LVNEAPVpYSVpYSK	STAM2	21 265 031	47.25	46.44	1.8E+08	1.2E+08	1.5	*	*
GPPQpSPVFEGVYNNSR	A2LP	27 262 649	47.43	47.11	1.8E+08	1.4E+08	1.3	*	*
NPQEGLpYNELQK	CD3 zeta	4 557 431	47.62	47.26	1.0E+08	1.2E+08	0.8	*	*
MAEApYSEIGMK	CD3 zeta	4 557 431	47.8	47.44	2.0E+07	2.1E+07	1.0		*
LQLDNQpYAVLENQK	hypothetical protein H41	8 923 710	48.34	47.82	7.0E+07	7.2E+07	1.0	*	*
pYETSSTSAGDRpYDSLLGR	MYPT1	4 505 317	48.53	48.17	4.0E+07	2.8E+07	1.4	*	*
ENDpYESISDLQQGR	PAG	7 682 684	48.89	48.49	2.2E+07	1.6E+07	1.4	*	*
AEFAEpYASVDR	Cbp/PAG	16 753 229	49.1	48.7	4.3E+07	1.7E+07	2.5	*	*
AQIPEGDpYLSYR	ERBIN	8 923 909	49.41	49.16	2.9E+07	1.5E+07	1.9	*	
pYSEVVLDSEPK	SIT	7 657 577	49.74	49.49	2.6E+08	2.6E+08	1.0	*	*
TGSpYGALAEITASK	protein phosphatase 1	4 505 317	50.25	ND	3.5E+07	ND	NA	*	
DEILPTpTPISEQK	S3 ribosomal protein	7 765 076	50.98	50.6	2.2E+07	5.0E+07	0.4	*	*
NEIIQpSPISQVPSVEK	endofin	7 662 048	51.54	51.1	4.6E+07	1.9E+07	2.4	*	
TLpSPTPpSAEGYQDVR	actin-binding DZF protein	2 337 952	52.35	51.52	1.4E+08	1.6E+08	0.9	*	*
pYQQPFEDFR	PLCg1	130 225	57.78	57.5	5.6E+07	6.0E+07	0.9	*	*
GQEGEpYAVPFDAVAR	p56dok	21 618 483	58.24	57.82	2.4E+08	4.2E+07	5.7	*	*
TTAVEIDYDpSLK	FYB	6 166 197	58.42	57.64	1.0E+08	5.8E+07	1.7	*	*
ApSFPDQApYANSQPAAS	SIT	7 657 577	58.42	57.64	4.7E+07	3.3E+07	1.4	*	*
TApSFGGITVLTR	similar to PP1, reg subunit 1c	30 354 625	58.42	57.97	8.1E+07	6.7E+07	1.2	*	*
pSPOLSDFGLER	RAMA1	27 448 171	58.97	58.57	4.8E+07	3.2E+07	1.5	*	*
SASQpSpSLDKLDQELK	JNK/SAPK associated protein	27 436 920	59.67	59.24	8.1E+07	3.2E+07	2.5	*	*
NEIIQpSPISQVPpSVEK	endofin	7 662 048	59.67	ND	3.5E+07	ND	NA	*	
IPGPGpTPVKpYSEVVLDSEPK	SIT	7 657 577	60	59.6	3.9E+07	3.2E+07	1.2	*	
RQpSILFSTEV	BCR	11 038 641	60.04	59.57	8.5E+07	4.4E+07	1.9	*	*
VTPPEGpYEVVTVFPK	LIMATIN	1 905 874	59.85	ND	3.4E+07	ND	NA	*	
LPSpSPVpYEDAASFK	Cortactin	2 498 954	60.4	59.75	4.6E+08	2.5E+08	1.8	*	*
TTAVEIDpYDpSLK	FYN binding protein	4 503 821	60.58	59.93	2.3E+07	2.5E+07	0.9	*	*
ALEVAEpYLTPVLK	Apg3p; PC3-96 protein	19 526 773	60.87	60.51	2.3E+07	1.0E+07	2.3	*	*
IpYDLNIPAFVK	NCK2	20 532 395	60.77	ND	2.2E+07	ND	NA	*	
SADAPApYQQGQNQLpYNELNLGR	CD3 zeta	4 557 431	61.19	60.58	3.9E+07	1.2E+07	3.3		*
SpSSPAPADIAQTVQEDLR	Ras-GAP binding protein 1	5 031 703	61.2	60.8	1.3E+08	2.1E+07	6.2	*	*

[a] Phosphorylation sites are shown in underlined text with pS representing a phosphoserine residue, pT representing a phosphothreonine residue, and pY representing a phosphotyrosine residue. If the exact phosphorylation site could not be defined, possible phosphorylated residues are shown in parentheses.
[b] Accession, NCBI accession number.
[c] RT = retention time (min); ND = not detected.
[d] Area = precursor peak area from ESI mass spectra with 1.7E+08 corresponding to 1.7×10^8.
[e] Fold difference = peak area from analysis 1/peak area from analysis 2; NA = not applicable.
[f] '*' signifies that an MS/MS spectrum was recorded for a peptide in the indicated analysis (1 or 2).

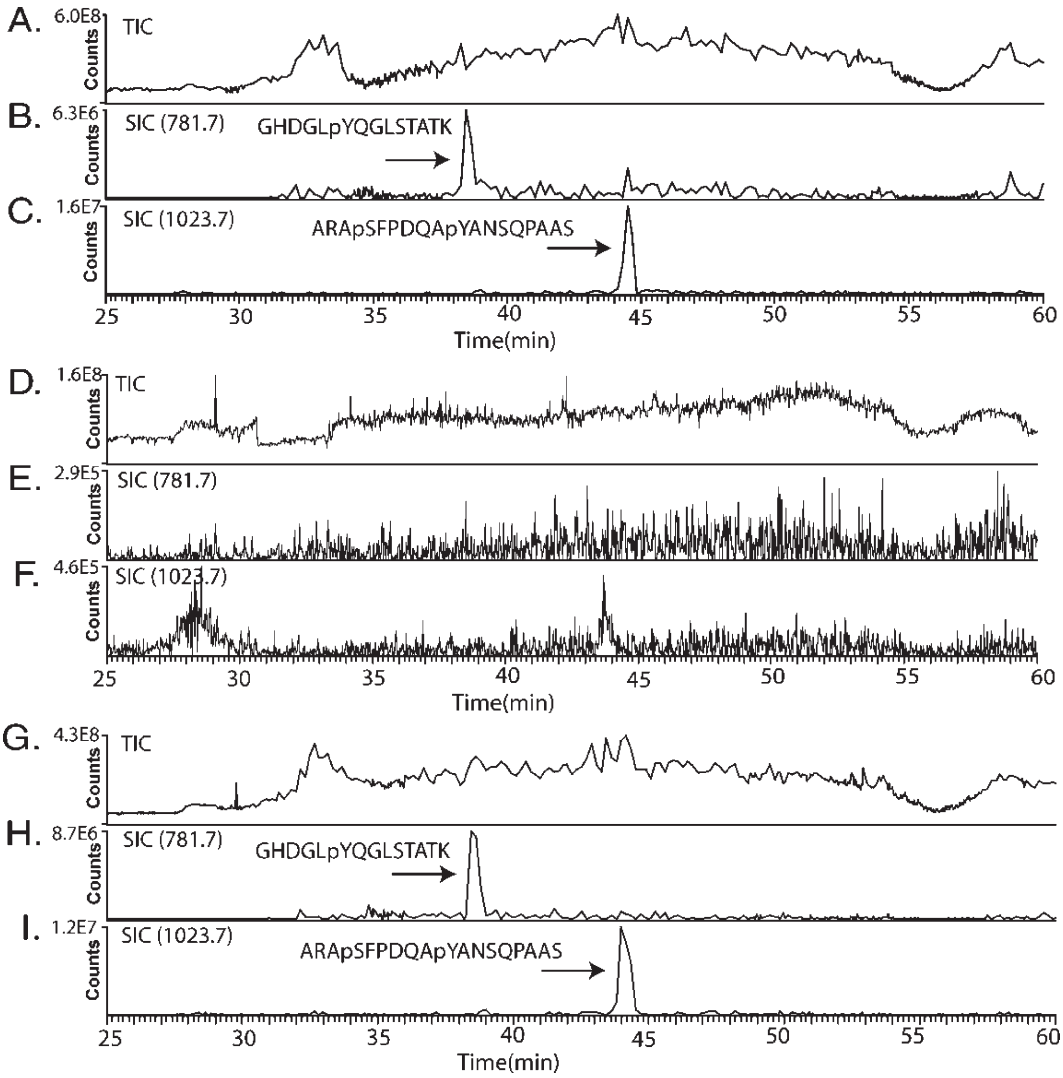

Figure 6. Complex mixtures were analyzed by desalt/IMAC/nano-LC/ESI-MS with little detectable carryover. (A, D, G) Total ion chromatograms (TICs) and (B, C, E, F, H, I) selected ion chromatograms (SICs) recorded for perdeuteromethylated phosphopeptides GHDGLpYQGLSTATK (B, E, H) and ARApSFPDQApYANSQPAAS (C, F, I) during replicate phosphoprofiling analyses of anti-phosphotyrosine immunoprecipitates of Jurkat T-cell lysates (clone PT66; analysis 1: A–C, analysis 2: G–I) or during blank injection performed after analysis 1 (D–F).

Automated analysis of proteins precipitated by different anti-phosphotyrosine antibody clones

As an illustration of the benefits of automated and robust sample processing, the desalt/IMAC/nano-LC/ESI-MS methodology was used to investigate the relative immunoprecipitation efficiencies of several commercially available anti-phosphotyrosine antibodies. Although the use of such antibodies is critical to studies that focus specifically on the analysis of the far less abundant phosphorylation of tyrosine residues compared to that of serine and threonine,[6,17,18,30] to our knowledge no reports address potential differences in abilities of such antibodies to precipitate phosphoproteins from complex mixtures. Accordingly, separate immunoprecipitations of proteins derived from a single pervanadate-stimulated Jurkat T-cell lysate were performed with antibody clones PT66, pY20 and 4G10. The immunoprecipitated proteins were digested, the resulting peptides converted into their methyl esters, and the esterified peptide mixtures were analyzed using the automated desalt/IMAC/nano-LC/ESI-MS platform. Blank injections across the entire fluidic pathway were performed in between each analysis to minimize carryover. As shown in Table 4, several tyrosine phosphorylated peptides were commonly identified in each of the three analyses. However, under these conditions, PT66 was found to be far superior to pY20 and 4G10 with respect to number of phosphorylated peptides identified and/or the overall quantity of enriched phosphopeptides. Thus, although clone 4G10 is routinely utilized for Western blotting experiments,[31] its excellent performance for this application does not necessarily imply similar levels of performance in immunoprecipitation experiments. It should be noted that further optimization of binding/elution conditions for pY20 or 4G10 may yield improved results for phosphoprofiling with these antibodies, and importantly, our system is uniquely suited to perform these studies as well.

Table 4. Peptide sequences and normalized peak areas of phosphopeptides observed in automated desalt/IMAC/nano-LC/ESI-MS profiling of immunoprecipitates from antibody clones 4G10, pY20, and PT66. Peak areas were measured using Xcalibur 1.3 software, and values normalized to LIEDAEpYTAK standard peak areas. Areas in normal print indicate peptides for which MS/MS data was acquired, while areas in bold correspond to peaks at correct retention times not identified by MS/MS. '0' indicates that the peptide was identified by MS/MS, but that the area of the peak could not be quantified due to a low S/N ratio. ND, not detected by MS or MS/MS

Peptide[a]	Protein name	Accession[b]	4G10	PY20	PT66	PT66/4G10*	PT66/PY20*
LPVDpYpYGIPFAAPTALASR	AD-012	22 325 364	ND	ND	0		
ADHRp(SS)PNVANQPPpSPGGK	AF6	12 644 018	**0.00292**	**0.00297**	0		
MILPpTKAMTQELTVKRK	AHA1	22 748 839	**0.00127**	0.00937	**0.06226**	48.9	6.6
RQpSILFSTEV	BCR	11 038 641	0.00100	**0.01189**	0.05920	59.2	5.0
IKPSSpSANAIpYSLAAR	CBL	115 855	ND	0	0.11671		
IKPSSpSANAIpYSLAARPLPVPK	CBL2	4 885 117	ND	0.02809	**0.40955**		14.6
KHYQPpYAPPR	CD28	5 453 611	ND	0.02845	ND		
NDQVpYQPLRDR	CD3d	4 502 669	ND	ND	0		
DLpYSGLNQR	CD3e	4 502 671	ND	0.09010	0.14357		1.6
ERPPPVPNPDpYEPIR	CD3e	4 502 671	**0.23695**	0.29802	0.75073	3.2	2.5
GHDGLpYQGLSTATK	CD3z	23 830 999	0	0.19901	0.14526		0.7
KNPQEGLpYNELQK	CD3z	23 830 999	ND	0	ND		
NPQEGLpYNELQK	CD3z	23 830 999	ND	0.04114	ND		
SADAPApYQQGQNQLpYNELNLGR	CD3z	4 557 431	0.00280	0.02674	0.23130	82.6	8.6
NEIIQpSPISQVPpSVEK	Endofin	7 662 048	ND	0.01072	0.12268		11.4
TpYVDPHTpYEDPTQAVHEFAK	EPA3	12 003 435	ND	0	ND		
STPpSHGSVSSLNSTGSLpSPK	Eps15R	10 864 047	ND	0.01135	0.17839		15.7
GPTSGPQSAPQIpYGPPQp(YNIQY)SSSAAVK	ERBIN	8 572 221	ND	0	0		
SKpSATLLpYDQPLQVFTGSSSSSDLISGTK	ERBIN	8 572 221	ND	0.00982	0.12284		12.5
GPTTGEGALDLSDVHpSPPKpSPEGK	FOP	5 901 954	ND	ND	0.17839		
TTAVEIDpYDSLK	FYB	6 166 197	0	0	0		
SSpSPAPADIAQTVQEDLR	G3BP	5 031 703	0.00303	0.05536	0.06519	21.5	1.2
RHpTDPVQLQAAGR	GADS	4 758 746	**0.00226**	0.89928	0.22713	100.7	0.3
HGpSGADp(SDY)ENTQSGDPLLGLEGK	GIT1	28 510 510	ND	ND	0		
LQPFHSTELEDDAIpYSVHVPAGLpYR	GIT1	28 510 510	ND	ND	0		
ILEADHFpYK	GSTM1-1	29 731 574	**0.08736**	0.01234	**1.17129**	13.4	94.9
LDQPVpSAPPpSPR	H4	22 477 628	ND	**0.06707**	0.12186		1.8
LQLDNQpYAVLENQK	Hyp Prot. H41	8 923 710	ND	0	ND		
pYIHLENLLAR	Hyp. Prot. FLJ10805	8 922 679	ND	**0.00883**	0.15611		17.7
LAPGSAGpSGSGSGSGGR	hyp.prot. FLJ11743	22 547 157	**0.00676**	0.74176	**0.82175**	121.6	1.1
WIPSIPPLQNHpSAVNR	hyp.prot.XP_209355	27 501 064	**0.23117**	0.28092	**0.73945**	3.2	2.6
SASQpSpSLDKLDQELK	JNK/SAPK AP	27 436 920	**0.00028**	**0.05230**	0.08204	293.3	1.6
PQAVGSSNpYASTSAGLK	KIAA0157	961 446	ND	0.00448	ND		
FSFYGNLpSPR	KIAA1389	7 243 159	ND	0	ND		
LTSSLLGMVAKNpSK	KIAA1856	27 662 574	**0.00087**	**0.00685**	0.21320	244.2	31.1
SVLEDFFTATEGQpYQPQP	LCK	6 984 209	ND	0.00838	0.04332		5.2
STLQDpSDEpYSNPAPLPLDQHSR	leupaxin	4 758 670	0.00522	**0.07840**	0.62540	119.8	8.0
VpSPGLPpSPNLENGAPAVGPVQPR	Lim domain ctg 1	13 548 632	ND	ND	0		
YYEGYpYAAGPGYGGR	LIM protein inlipoma	5 031 887	0.01498	0.13420	0.41095	27.4	3.1

TLpSPTPpSAEGYQDVR	Limatin	21 284 387	0	0	ND		
TSSESIpYSRPGSSIPGSPGHpTIYAK	limatin	21 284 383	0	**0.03988**	**0.11950**		3.0
VADPDHDHTGFLpTEpYVATR	MAPK	23 879	**0.00410**	ND	0.07855	19.2	
RYPp(SS)ISp(SS)PQKDLTQAK	NICE-4	7 661 942	0	0	0.09958		
RYPSSIpp(SSS)PQKDLTQAK	NICE-4	7 661 942	0.00597	0	0		
RYPSSISSpSPQK	NICE-4	7 661 942	0.00085	**0.03519**	0.01143	13.4	0.3
RYPSSISSpSPQKDLTQAK	NICE-4	7 661 942	0	0.02872	0		0.0
SPAVATSTAAPPPPp(SS)PLPSK	NICE-4	7 661 942	ND	ND	0		
GQEGEpYAVPFDAVAR	p56dok	4 503 359	0.00128	0.01675	ND		
EDPIpYDEPEGLAPVPPQGLpYDLPR	p56dok	4 503 357	ND	0	**0.03078**		
LPSPPGPGELLDpSPPALpYAEPLDSLR	p62dok	4 503 357	ND	0.01693	0.10487		6.2
SHNSALpYSQVQK	p62dok	4 503 357	0.01466	0	**0.15471**	10.6	
VKEEGpYELPYNPATDDpYAVPPPR	p62dok	4 503 357	0.00826	**0.47894**	**1.20331**	145.7	2.5
pYREPPPpTPPGYLGISLADLK	PDZ-GEF2	20 386 206	ND	0.04384	ND		
TYpYSPVYR	Plakophilin 4	29 791 421	ND	0	ND		
AASPp(YS)QRPApSPTAIR	Plakophillin 4	29 791 421	0	0.05212	ND		
SAVpSPDLHITPIpYEGR	Plakophillin 4	29 791 421	0	0	ND		
pYQQPFEDFR	PLCg1	130 225	0.00135	0.02179	0.06727	49.9	3.1
DINSLpYDVSR	PLCg2	4 505 871	ND	0	0		
p(SS)GTASSVAFpTPLQGLEIVNPQAAEK	pre-mRNA PF 31 hlg	7 661 654	ND	0	0.06002		
PSQGLPVIQpSPPSpSPPHR	Putative ankyrin repeat cont. prot.	16 076 877	**0.00111**	0.07418	**0.02912**	26.2	0.4
ASpSFSGISVLTR	R3HD	7 661 874	ND	ND	0		
KLpSGDQITLPTTVDpYSSVPK	RCAS	4 758 230	ND	0.01783	0.09373		5.3
KLSGDQIpTLPTTVDpYSSVPK	RCAS	4 758 230	ND	0.01648	ND		
ASSFpSGISVLTR	RH3 domain	31 543 535	ND	0	ND		
p(SSS)LSAANTSQTNPQGAVSSTVSGLQPRQpSK	RhoGEF6	22 027 525	ND	0	0.12242		
YSPTpSPTpYSPTSPK	RNA Pol II largest subunit	4 505 939	ND	ND	0.13243		
p(YY)DSRPGGYGYGYGR	RNAbp3	5 803 137	0.00137	**0.03789**	**0.06420**	46.8	1.7
YpYDSRPGGYGYGYGR	RNAbp3	5 803 137	ND	0.01630	0.32739		20.1
YDERPGPpSPLPHR	RU17	88 959	ND	ND	0.01157		
NpYGSpYSTQASAAAATAELLK	SCA3	16 445 419	ND	0	0.07076		
QpYATLDVYNPFETR	SCA3	16 445 419	0	0.07859	0.13328		1.7
TGDLGIPPNPEDRpSPpSPEPIYNSEGKR	SF1B	7 513 392	ND	0.03889	ND		
HRPpSPPApTPPPK	Sim to Ser/Arg repetitive matrix 1	23 274 133	**0.00068**	0.00094	0.00609	9.0	6.5
ARApSFPDQApYANSQPAAS	SIT	7 657 577	0.00241	0.08650	0.82593	342.1	9.5
IPGPGpTPVKpYSEVVLDSEPK	SIT	7 657 577	0	0.14140	0.45133		3.2
IPGPTPVKpYPSEVVLDSEPK	SIT	7 657 577	0.00830	0.13960	2.07631	250.1	14.9
pYSEVVLDSEPK	SIT	7 657 577	0.00159	0.02529	0.06003	37.8	2.4
SGEpSVEEVPLpYGNLHYLQTGR	SIT	7 657 577	0.00273	**0.01629**	0.46386	169.9	28.5
SGESVEEVPLpYGNLHpYLQTG	SIT	7 657 577	**0.00218**	**0.01899**	**0.40524**	186.1	21.3
NHpSPLPPPQTNHEEPSR	SLP-76	5 031 855	ND	ND	0		
LVNEAPVpYSVpYSK	STAM2	21 265 031	ND	0	**0.08509**		
p(TRS)GFEGGApTKPVADVALLGPRFSGYDpSVR	Unk (prot. for IMAGE:4831224)	21 961 508	ND	0.00837	ND		
ALGADDSYpYTAR	ZAP-70	1 177 044	ND	0.05743	0.14357		2.5
IDTLNpSDGpYTPEPAR	ZAP-70	1 177 044	ND	**0.02439**	ND		
IDTLNSDGpYTPEPAR	ZAP-70	1 177 044	ND	0.05950	0.08705		1.5
RIDTLNpSDGpYTPEPAR	ZAP-70	1 177 044	**0.00518**	0.05230	**0.10876**	21.0	2.1

Continues

Table 4. Continued

Peptide[a]	Protein name	Accession[b]	4G10	PY20	PT66	PT66/4G10*	PT66/PY20*
RIDTLNSDGpYTPEPAR	ZAP-70	1 177 044	ND	0.10900	0.16446		1.5
AYDPDpYERAYpSPEYR	ZO-2a	5 924 410	ND	ND	0.05641		
					Mean:	91.4	8.9

[a] Phosphorylation sites are shown in underlined text with pS representing a phosphoserine residue, pT representing a phosphothreonine residue, and pY representing a phosphotyrosine residue. If the exact phosphorylation site could not be defined, possible phosphorylated residues are shown in parenthesis.
[b] Accession, NCBI accession number.
*Ratio of peak areas from indicated analyses, when defined.

CONCLUSIONS

We have implemented a versatile system for performing nano-LC/ESI-MS experiments with or without IMAC enrichment in a fully automated fashion. Additional features include robust analytical columns with integrated emitter tips (<5 μm i.d.) and automated peak parking to flow rates near 30 nL/min. Such automated sample processing will be especially important to studies that require high-sensitivity IMAC analysis of numerous gel-derived samples, multiple time points or cellular compartments, different enzymatic digestions for maximum protein coverage, or when replicates are necessary to derive statistical data. It should be noted that this platform could readily be implemented with different mass spectrometers (e.g. ESI-QTOFMS for accurate mass measurements) or in conjunction with electron transfer dissociation to enable the fragmentation of phosphopeptides without the neutral loss of phosphoric acid.[32] Although IMAC was specifically investigated in this study, the platform could be utilized with numerous other enrichment methodologies. For example, the metal-chelating media could easily be replaced with strong cation-exchange,[33] titanium oxide,[34] or other affinity resins depending on the desired application. Due to its ability to enrich phosphorylated peptides from both simple as well as complex mixtures, this versatile system could be utilized to study phosphorylation in many different cellular systems in a truly high-throughput manner.

Acknowledgements

We thank the Genomics Institute of the Novartis Research Foundation (GNF) and Dr. Peter G. Schultz for generous support.

Note: Visual Basic source code, HPLC sequences and methods, and MS methods will be supplied by the authors upon request.

REFERENCES

1. Manning G, Whyte DB, Martinez R, Hunter T, Sudarsanam S. *Science* 2002; **298**: 1912.
2. Pawson T, Scott JD. *Science* 1997; **278**: 2075.
3. Mann M, Ong SE, Gronborg M, Steen H, Jensen ON, Pandey A. *Trends Biotechnol*. 2002; **20**: 261.
4. Holmberg CI, Tran SE, Eriksson JE, Sistonen L. *Trends Biochem. Sci*. 2002; **27**: 619.
5. McLachlin DT, Chait BT. *Curr. Opin. Chem. Biol*. 2001; **5**: 591.
6. Soskic V, Gorlach M, Poznanovic S, Boehmer FD, Godovac-Zimmermann J. *Biochemistry* 1999; **38**: 1757.
7. Marcus K, Immler D, Sternberger J, Meyer HE. *Electrophoresis* 2000; **21**: 2622.
8. Muszynska G, Dobrowolska G, Medin A, Ekman P, Porath JO. *J. Chromatogr*. 1992; **604**: 19.
9. Nuwaysir L, Stults J. *J. Am. Soc. Mass Spectrom*. 1993; **4**: 662.
10. Watts JD, Affolter M, Krebs DL, Wange RL, Samelson LE, Aebersold R. *J. Biol. Chem*. 1994; **269**: 29520.
11. Posewitz MC, Tempst P. *Anal. Chem*. 1999; **71**: 2883.
12. Gioeli D, Ficarro SB, Kwiek JJ, Aaronson D, Hancock M, Catling AD, White FM, Christian RE, Settlage RE, Shabanowitz J, Hunt DF, Weber MJ. *J. Biol. Chem*. 2002; **277**: 29304.

13. Ficarro SB, McCleland ML, Stukenberg PT, Burke DJ, Ross MM, Shabanowitz J, Hunt DF, White FM. *Nat. Biotechnol.* 2002; **20**: 301.
14. Ficarro S, Chertihin O, Westbrook VA, White F, Jayes F, Kalab P, Marto JA, Shabanowitz J, Herr JC, Hunt DF, Visconti PE. *J. Biol. Chem.* 2003; **278**: 11579.
15. Nuhse TS, Stensballe A, Jensen ON, Peck SC. *Mol. Cell Proteomics* 2003; **2**: 1234.
16. Shu H, Chen S, Bi Q, Mumby M, Brekken DL. *Mol. Cell Proteomics* 2004; **3**: 279.
17. Brill LM, Salomon AR, Ficarro SB, Mukherji M, Stettler-Gill M, Peters EC. *Anal. Chem.* 2004; **76**: 2763.
18. Salomon AR, Ficarro SB, Brill LM, Brinker A, Phung QT, Ericson C, Sauer K, Brock A, Horn DM, Schultz PG, Peters EC. *Proc. Natl. Acad. Sci. USA* 2003; **100**: 443.
19. Riggs L, Sioma C, Regnier FE. *J. Chromatogr. A* 2001; **924**: 359.
20. Valaskovic GA, Kelleher NL, Little DP, Aaserud DJ, McLafferty FW. *Anal. Chem.* 1995; **67**: 3802.
21. Wilm M, Mann M. *Anal. Chem.* 1996; **68**: 1.
22. Haskins WE, Wang Z, Watson CJ, Rostand RR, Witowski SR, Powell DH, Kennedy RT. *Anal. Chem.* 2001; **73**: 5005.
23. Licklider LJ, Thoreen CC, Peng J, Gygi SP. *Anal. Chem.* 2002; **74**: 3076.
24. Martin SE, Shabanowitz J, Hunt DF, Marto JA. *Anal. Chem.* 2000; **72**: 4266.
25. Secrist JP, Burns LA, Karnitz L, Koretzky GA, Abraham RT. *J. Biol. Chem.* 1993; **268**: 5886.
26. Cortes HJ, Pfeiffer CD, Richter BE, Stevens TS. *J. High Res. Chromatogr. Chromatogr. Commun.* 1987; **10**: 446.
27. Eng J, McCormack A, Yates JR. *J. Am. Soc. Mass Spectrom.* 1994; **5**: 976.
28. Davis MT, Stahl DC, Hefta SA, Lee TD. *Anal. Chem.* 1995; **67**: 4549.
29. Zarling AL, Ficarro SB, White FM, Shabanowitz J, Hunt DF, Engelhard VH. *J. Exp. Med.* 2000; **192**: 1755.
30. Steen H, Kuster B, Fernandez M, Pandey A, Mann M. *J. Biol. Chem.* 2002; **277**: 1031.
31. Druker BJ, Mamon HJ, Roberts TM. *New Eng. J. Med.* 1989; **321**: 1383.
32. Syka JE, Coon JJ, Schroeder MJ, Shabanowitz J, Hunt DF. *Proc. Natl. Acad. Sci. USA* 2004; **101**: 9528.
33. Wolters DA, Washburn MP, Yates JR III. *Anal. Chem.* 2001; **73**: 5683.
34. Pinkse M, Uitto P, Hilhorst M, Ooms B, Heck A. *Anal. Chem.* 2004; **76**: 3935.